crystals

MDPI

Article

Study on the Simulation and Experimental Impact of Substrate Holder Design on 3-Inch High-Quality Polycrystalline Diamond Thin Film Growth in a 2.45 GHz Resonant Cavity MPCVD

Shuai Wu [1], Kesheng Guo [2,*], Jie Bai [3], Jiafeng Li [2], Jingming Zhu [2], Lei Liu [3], Lei Huang [2], Chuandong Zhang [3] and Qiang Wang [1,3,*]

[1] School of Materials Science and Engineering, Chongqing Jiaotong University, Chongqing 400074, China
[2] Jihua Laboratory, Foshan 528200, China
[3] School of Aeronautics, Chongqing Jiaotong University, Chongqing 400074, China
* Correspondence: guoks@jihualab.com (K.G.); wangq@cqjtu.edu.cn (Q.W.)

Abstract: In this study, three different substrate holder shapes—trapezoidal, circular frustum, and adjustable cyclic—were designed and optimized to enhance the quality of polycrystalline diamond films grown using microwave plasma chemical vapor deposition (MPCVD). Simulation results indicate that altering the shape of the substrate holder leads to a uniform distribution of the electric field on the surface, significantly suppressing the formation of secondary plasma. This design ensures a more even distribution of the temperature field and plasma environment on the substrate holder, resulting in a heart-shaped distribution. Polycrystalline diamond films were synthesized under these three different substrate holder conditions, and their morphology and crystal quality were characterized using optical microscopy, Raman spectroscopy, and high-resolution X-ray diffraction. Under conditions of 5 kW power and 90 Torr pressure, the adjustable cyclic substrate holder produced high-quality 3-inch diamond films with low stress and narrow Raman full width at half maximum (FWHM). The results confirm the reliability of the simulations and the effectiveness of the adjustable cyclic substrate holder. This approach provides a viable method for scaling up the size and improving the quality of polycrystalline diamond films for future applications.

Keywords: 2.45 GHz; MPCVD; polycrystalline diamond thin film; design of substrate holder; numerical simulation

Citation: Wu, S.; Guo, K.; Bai, J.; Li, J.; Zhu, J.; Liu, L.; Huang, L.; Zhang, C.; Wang, Q. Study on the Simulation and Experimental Impact of Substrate Holder Design on 3-Inch High-Quality Polycrystalline Diamond Thin Film Growth in a 2.45 GHz Resonant Cavity MPCVD. *Crystals* **2024**, *14*, 821. https://doi.org/10.3390/cryst14090821

Academic Editor: Dah-Shyang Tsai

Received: 19 August 2024
Revised: 10 September 2024
Accepted: 14 September 2024
Published: 20 September 2024

1. Introduction

The development of wide-bandgap semiconductor materials such as SiC [1], GaN [2], and AlN [3] has revolutionized various fields, including microelectromechanical systems, aerospace materials, information sensing, acoustic filters, and quantum technology [4,5]. These materials are favored because of their high breakdown electric fields, electron mobility, and excellent environmental stability. However, operating at higher power levels presents significant challenges owing to heat-dissipation issues, which limit performance and compromise device reliability. Effective thermal management is essential for addressing this challenge. Diamond has emerged as a highly promising material for thermal management because of its extremely high thermal conductivity (2000 W/mK), high radiation hardness, and excellent chemical stability [6]. Integrating diamond with wide-bandgap semiconductors can enhance heat dissipation, thereby increasing the area-dissipation density and reducing the working-channel temperature. This integration offers a viable solution to improve the performance and reliability of devices operating at high power levels [7].

Various chemical vapor deposition (CVD) techniques have been employed to deposit large-area, high-quality polycrystalline diamond films. These high-quality films are generally characterized by a low residual stress, fewer defect peaks, absence of impurity

phases, and high crystallinity. This process typically involves the reaction of a mixture of gases (e.g., CH_4 and H_2) on a substrate, resulting in the formation of polycrystalline diamond films [8,9]. Currently, MPCVD is the most refined method for producing synthetic diamonds. A mixture of gases (hydrogen and carbon source gases) is introduced, and the microwaves generated by the microwave source are transmitted through a rectangular waveguide. After passing through a mode converter, the microwaves are coupled to the resonant cavity. A microwave resonator creates a strong and uniform standing-wave electric field that ionizes gases to form a plasma ball [10]. The substrate is placed beneath the plasma ball for the diamond film growth. This electrode-free process eliminates potential contamination sources, enabling the deposition of high-quality polycrystalline diamond films on the substrate. The resonant cavity in MPCVD equipment is characterized by microwave resonance. When microwaves of the resonant frequency are input into the cavity, resonance occurs, creating a high-intensity electric field. This electric field can be adjusted by modifying the size and shape of the cavity to achieve an optimal electric field distribution and generate a plasma ball at a specific location. However, this requires high precision in cavity machining because the presence of plasma also affects the resonant cavity. Therefore, to optimize the design of the resonant cavity, it is necessary to simulate the electric field and calculate the plasma distribution [11,12].

The process of growing high-quality polycrystalline diamond thin films is influenced by numerous parameters, including substrate selection [13], microwave power [14], chamber pressure [15], gas composition [16], chamber temperature [17], plasma ball density [18], and substrate support [19]. Additionally, the cavity size and frequency of MPCVD equipment play significant roles. Currently, the MPCVD frequencies used are 915 MHz and 2.45 GHz. When comparing microwaves of two different frequencies, the 915 MHz frequency has a longer wavelength, resulting in a larger plasma ball. Consequently, the required microwave power is higher, leading to a larger diameter of deposited diamond film. However, MPCVD equipment operating at 915 MHz demands higher power, making the structure and details of the equipment more complex and posing significant challenges for maintaining vacuum conditions [20,21]. This, in turn, increases the requirements for equipment development, manufacturing technology, and cost. On the other hand, MPCVD operating at 2.45 GHz can achieve high plasma density and deposition rates and has been widely adopted. In general, when microwaves are coupled to a resonant cavity, two resonance modes exist: transverse electric (TE) and transverse magnetic (TM). The inner metal walls of the cavity enforce a zero-tangential component on the electric field, causing it to be perpendicular to the inner wall surface. In the TE mode, there are no strong electric field regions in contact with the metal, meaning the plasma cannot contact the substrate surface. Therefore, the TM mode is commonly used, with TM_{0mn} being the most prevalent (where 0 indicates an axially symmetric surface electric field structure, and m and n represent the number of axial and radial electric field maxima in the resonant cavity, respectively). Moreover, the substrate holder within the cavity plays a crucial role in the effective utilization of microwave energy [22–24]. To ensure maximum energy utilization, a substrate holder is added to the reaction zone to focus the electric field above the substrate, thereby avoiding the formation of secondary electric fields. In 2017, An et al. [25] observed that reducing the substrate support size radially and increasing it axially resulted in an uneven plasma distribution. They discovered that altering the height of the movable substrate could achieve uniform plasma and power density. In 2022, a T-shaped substrate was developed, introducing a gap at the edge that created a strong additional electric field, enhancing the edge temperature uniformity and improving the quality of the deposited polycrystalline diamond films. Zhao et al. [26] simulated and introduced a hole in the center of the substrate stage and found that it suppressed nitrogen gas in the cavity without significantly affecting the plasma, although the electron density decreased by 40%. Sedov et al. [19] designed three different geometric shapes for substrate platforms using electric field simulations and manufactured two-inch polycrystalline diamond thin films through simulation testing. However, these platforms exhibited strong edge effects.

In this study, a butterfly-shaped resonant cavity was employed within a frequency-domain transient solution mode, coupled with multiple physical fields. Various substrate holder designs were proposed to investigate their impact on the microwave electric field, plasma environment, and the quality of diamond films. Numerical simulations and experimental tests were conducted to identify the optimal substrate holder for the deposition of high-quality diamond.

2. Simulation and Experiment

2.1. Simulation Modeling

Figure 1a shows a schematic of the butterfly resonant cavity MPCVD used in the experiment. Using quartz as the dielectric window, this setup can be classified as a quartz-ring MPCVD, which is a non-cylindrical plasma device. Microwaves are input from below, coupled into the stainless-steel reaction chamber through a quartz window, and focused above the substrate stage to form a strong electric field. At the bottom of the cavity, there is a single substrate holder with a width of 220 mm for placement of the substrate. The remaining dimensions are shown in Figure 1a. The electric field distribution in Figure 1b shows a strong secondary electric field near the top of the cavity. At high power, this can lead to the formation of secondary plasma, resulting in capability loss.

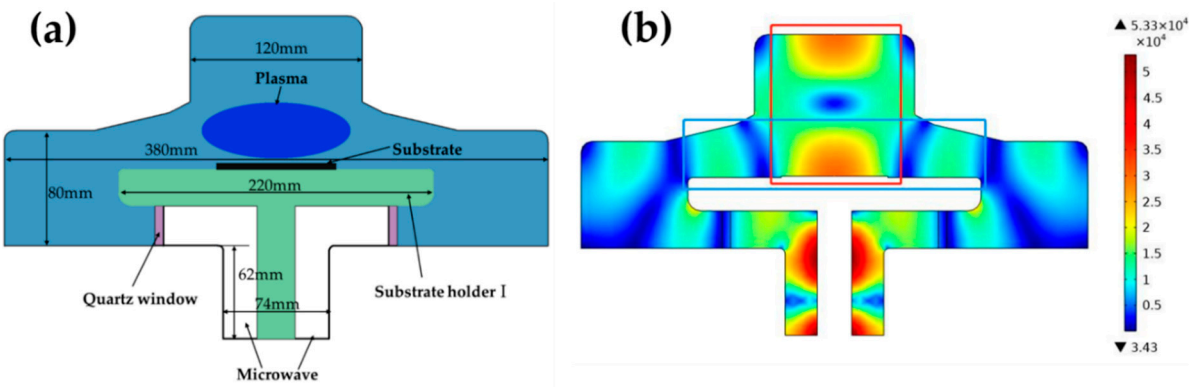

Figure 1. (**a**) Schematic diagram of a 2.45 GHz butterfly resonant cavity MPCVD and (**b**) electric field distribution without plasma generation at an input power of 1.5 kW.

To address the issue of secondary plasma formation and achieve high-quality polycrystalline diamond films, we designed three different substrate holders to suppress secondary plasma. In addition, we developed a substrate platform that ensures a highly uniform plasma field distribution. Figure 2 shows a schematic diagram of the three substrate holders, all made of Mo. These holders were designed to tune microwaves, adjust electric fields, and optimize plasma and temperature distribution.

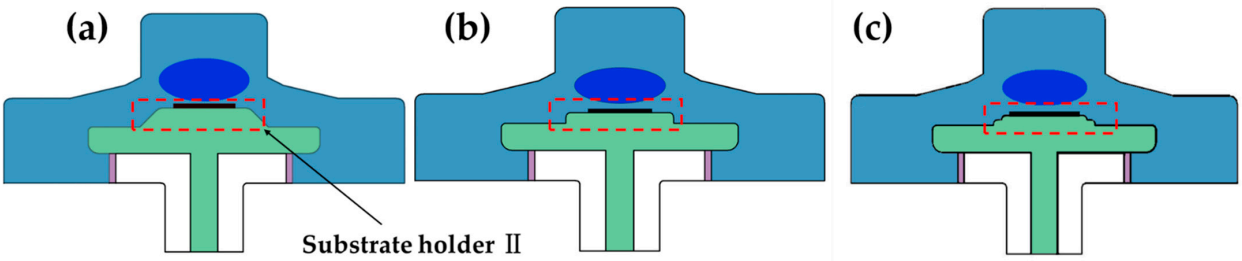

Figure 2. The three designed substrate holders display (**a**) trapezoidal, (**b**) circular frustum, and (**c**) adjustable cyclic shapes in the red box.

To simulate the experimental process, a finite element analysis method was used to study the electric field and plasma electron density distribution inside the cavity. During the simulation, we used a microwave power of 1000 W, working pressure of 40 Torr,

and microwave frequency of 2.45 GHz. The plasma model approximates the Boltzmann equation by using a fluid equation. The rate of change in the electron density can be described by Equation (1):

$$\frac{\partial}{\partial t}(n_e) = R_e + \nabla \cdot \Gamma_e \quad (1)$$

In the formula, Γ_e is the electron flux, and R_e is the electron source.

The definition of electron flux Γ_e is as follows:

$$\Gamma_e = \mu_e n_e E + \nabla(D_e n_e) \quad (2)$$

The electronic source R_e is defined as

$$R_e = \sum_{j=1}^{M} x_j k_j N_n n_e \quad (3)$$

where x_j is the molar fraction of the target substance for reaction j, k_j is the rate constant for reaction j, and N_n is the total number density of neutral particles.

The rate of change of electron energy density is

$$\frac{\partial}{\partial t}(n_\varepsilon) = R_\varepsilon + \nabla \cdot \Gamma_\varepsilon + E \cdot \Gamma_e \quad (4)$$

where n_ε is the electron energy density, and R_ε is the loss or increase in ability caused by inelastic collisions. Γ_ε is defined as the electron energy flux:

$$\Gamma_\varepsilon = \mu_\varepsilon n_\varepsilon E + \nabla(D_\varepsilon n_\varepsilon) \quad (5)$$

The microwave electric field distribution of the MPCVD device is solved by Maxwell's equation:

$$\nabla \times \mu_r^{-1}(\nabla \times E) - k_0^2\left(\epsilon_r - \frac{j\sigma}{\omega\epsilon_0}\right)E = 0 \quad (6)$$

In the formula, E is the electric field, ω and k_0 are the angular frequency and wavenumber of microwaves, ϵ_0 is the vacuum dielectric constant, μ_r, ϵ_r, and σ are the relative magnetic permeability, relative dielectric constant, and conductivity of the material, respectively, and j is the imaginary unit. In the non-discharged gas region, $\epsilon_r = 1$, $\sigma = 0$; in the quartz glass region, $\epsilon_r = 3.78$, $\sigma = 0$; and for the discharged gas region, the conductivity is given by the following formula:

$$\sigma = \frac{n_e q^2}{m_e(\nu_e + j\omega)} \quad (7)$$

In the formula, q and m_e are the charge and mass of electrons, respectively, n_e is the electron density, and ν_e is the electron neutral particle collision frequency of the plasma.

During the diamond deposition process, the introduction of a small amount of methane does not have a significant impact. Therefore, only the discharge process of H_2 is considered. The hydrogen plasma reaction was studied based on the work of K. Hassouni [27]. Our model includes only e, H_2, H, H (n = 2), H (n = 3), H_+, and H_2^+. In the calculations, the gas temperature is set to be equal to the ion temperature. The following are some important H_2 plasma reactions:

$$e + H_2 \rightarrow 2e + H_2^+ \quad (R1)$$

$$e + H \rightarrow e + H^* \quad (R2)$$

$$e + H_2 \rightarrow e + 2H \quad (R3)$$

$$e + H_2 \rightarrow e + H_2 \quad \text{(R4)}$$

$$H_2^+ + H \rightarrow H^+ + H_2 \quad \text{(R5)}$$

$$H^{**} \rightarrow H + hv \quad \text{(R6)}$$

The electronic energy loss R_ϵ is obtained by summing up the collision energy losses of all reactions:

$$R_\epsilon = \sum_{j=1}^{p} x_j k_j N_n n_e \Delta\epsilon_j \quad (8)$$

In the equation, $\Delta\epsilon_j$ is the energy loss of reaction j. The reaction rate was calculated using reaction collision cross-section data and the electron energy distribution function:

$$k_j = \gamma \int_0^\infty \epsilon \sigma_k(\epsilon) f(\epsilon) d\epsilon \quad (9)$$

Among them , $\gamma = \sqrt{2q/m}$, $\sigma_k(\epsilon)$ is the collision cross-section, and $f(\epsilon)$ is the electron energy distribution function (EEDF).

In addition, the simulation of MPCVD equipment must also consider the impact of gas temperature, assuming the effects of convection are negligible:

$$\nabla \cdot (-k \nabla T_g) = Q \quad (10)$$

In the equation, k represents the thermal conductivity of the gas, T_g is the gas temperature, and Q denotes the heat source of the gas. In the MPCVD device, the average free path of electrons is very short, and the ability of electrons to absorb from microwaves is transferred to the gas in a short period of time, causing the gas temperature to rise. Therefore, when calculating, the heat source Q can be approximated as the power density Q_h.

2.2. Experimental Details

Polycrystalline diamond thin films were deposited on a 3-inch monocrystalline silicon (100) substrate. Before diamond deposition, the Si substrate was immersed in a nanodiamond suspension and sonicated for 30 min to enhance the diamond nucleation capability. After drying, the substrates were prepared for diamond growth. The processed silicon substrate was then placed on three differently designed deposition supports in alignment with the simulated configurations. The growth conditions were set as follows: microwave power of 5 kW, pressure of 90 Torr, and H_2/CH_4 flow rates of 300 and 9 sccm, respectively. By comparing the properties of the grown polycrystalline diamond films with the simulation results, the optimal substrate support for achieving high-quality polycrystalline diamond films was identified.

An infrared thermometer was used to measure the temperatures of the substrate support and Si during the deposition process through a window at the top of the cavity. High-resolution field-emission scanning electron microscopy (FE-SEM; Verios 5 UC, Thermo Fisher, Brno, Czech Republic) was used to examine the surface morphology of the polycrystalline diamond films. Additionally, a confocal laser Raman microscope (Renishaw in Via Qontor, argon ion laser, London, UK, 514.5 nm, 50 mW, spectral resolution ≤ 1 cm^{-1}) was utilized to analyze the structural information of defects and deposits within the polycrystalline diamond films.

3. Results and Discussion

3.1. Influence of the Substrate Holder on the Electric Field in the Cavity

First, through simulation, we calculated the electric field distribution inside the cavity for different substrate holders. Studying the influence of electric fields before plasma generation is crucial. As shown in Figure 3a, two strong electric field regions appear in the cavity: one at the top of substrate holder I and the other at the top of the cavity. In this

scenario, the electric field strength is very low and has a wide distribution range, which is extremely unfavorable for plasma generation. The presence of two electric fields within the cavity causes energy loss, resulting in an ineffective utilization of the input power for diamond deposition.

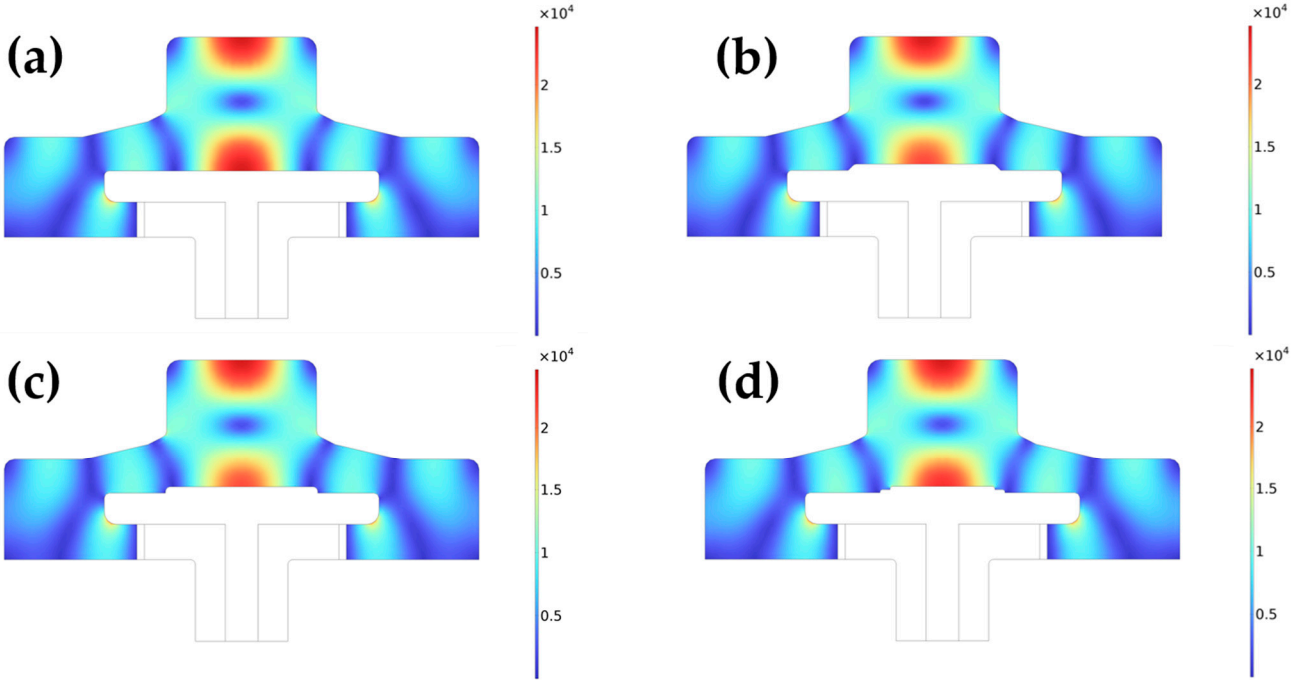

Figure 3. Electric field distribution diagram (V/m) of the MPCVD device with complete TM_{011} and TM_{021} modes, (**a**) no substrate holder II, (**b**) trapezoidal, (**c**) circular frustum, and (**d**) adjustable cyclic shape.

To enhance electric field utilization and reduce energy loss, Li et al. [28] added a splitter at the top of the cavity to shield the electric field focusing at the top, retaining only the strong electric field above the substrate stage inside the cavity. However, this design does not allow real-time adjustment of the substrate stage position, resulting in poor coordination. To address this issue, Zhang et al. [29] designed a cylindrical cavity by inverting it by 180°, which shields the electric field area above and concentrates the strong electric fields below the cavity for substrate placement. By optimizing the cavity parameters, they achieved a single high-density plasma sphere; however, this design only allowed the preparation of two-inch high-quality polycrystalline diamond films.

Compared with traditional cylindrical cavities, the butterfly resonant cavity in this study can generate a larger electric field and plasma size, which is beneficial for the large-scale and high-quality deposition of diamonds. To suppress the secondary electric fields, we propose three different substrate holders; their electric field distributions are shown in Figure 3. Previous studies have shown that placing a sample in a pocket-like substrate holder can protect the edges of the sample but results in an uneven electric field distribution [19]. Another study [30] suggested that increasing the height of the pocket substrate holder can improve the electric field, thereby enhancing the quality of the polycrystalline diamond films. Conversely, taller substrate holders demonstrate better electric field uniformity. In this study, we propose a trapezoidal substrate holder as shown in Figure 3b. The dimensions are 122 mm at the bottom, 5 mm in height, and 78 mm at the top with chamfered edges. A significant increase in the electric field intensity was observed, reaching 3.4×10^4 V/m. The electric field at the upper bottom of the trapezoidal holder weakened, and the strongest lateral electric field intensity was observed at the top of the cavity. Additionally, a strong edge effect was generated at the lower end of the original substrate holder, causing damage to the holder and resulting in electric field energy loss.

To address these issues, we propose a second type of substrate holder, II, designed as a circular frustum with a bottom diameter of 100 mm, an upper diameter of 90 mm, and a height of 5 mm, featuring chamfered edges. As shown in Figure 3c, this design reduces the edge effect observed at the lower end of the initial substrate holder, achieving an electric field intensity on the circular frustum of up to 4.4×10^4 V/m. Despite this improvement, the design exhibits an uneven electric field and lacks the ability to move vertically, which is crucial for adjusting the geometric shape of the resonant cavity and achieving optimal coordination. To enhance the design further, a lifting cylinder was added to the middle of the substrate holder. Figure 3d illustrates this improved design, which includes a circular platform with an upper diameter of 88 mm, a lower diameter of 100 mm, and a height of 5 mm. The movable cylinder, with a diameter of 78 mm, can be adjusted within an 8 mm range. This adjustment capability allowed for the coordination of the electric field during the growth process, resulting in a uniform electric field with a maximum intensity of 1.5×10^5 V/m.

3.2. Influence of the Substrate Holder on Plasma Electron Density in the Cavity

To better understand the influence of the substrate structure on the preparation of high-quality polycrystalline diamond films, it is essential to calculate not only the electric field distribution within the cavity but also the plasma electron density distribution. The principle of the resonant cavity involves focusing the electric field to excite the precursor gases, thereby forming a plasma [31]. In addition, the presence of plasma affects the electric field distribution, making the simulation of the plasma electron density distribution crucial [32]. A finite element method was employed to simulate plasma behavior in the butterfly cavity. To obtain reliable results, a simulation time of 2 s was selected for the plasma model calculations. This duration ensured the convergence of the model, providing accurate and consistent plasma electron density distribution data. The results of these simulations are essential for optimizing the substrate holder design, ultimately leading to the production of high-quality polycrystalline diamond films.

Figure 4 shows the plasma electron density distribution maps ($1/m^3$) for four different substrate holders. During operation of the MPCVD cavity, the electric field generates a secondary plasma electron located at the top of the cavity. This secondary plasma electron produces a shielding effect that weakens the plasma electrons above the substrate, hindering the high-quality deposition of polycrystalline diamond films [33]. The plasma electron density distribution is crucial in MPCVD because it directly affects the uniformity and rate of the deposition process. Figure 4a shows the plasma electron density distribution without the substrate holder II. A high-density plasma region is generated at the center of the substrate holder, with a maximum of 7.41×10^{17} m^{-3}, and the density decreases outward from the center. Under these conditions, the deposition rate at the center of the substrate was high, whereas that at the edges it was low, resulting in inconsistent and uneven diamond growth rates. Additionally, the heating temperature of the substrate inside the cavity is entirely from the plasma electrons and is too low for the optimal growth of polycrystalline diamonds. Figure 4b shows the plasma electron density distribution of the trapezoidal substrate holder II. The plasma electron density on the substrate holder decreases significantly, but a smaller plasma region is generated below the substrate holder. The secondary plasma electron density at the top of the cavity increases, which is unfavorable for the growth of polycrystalline diamond [34]. Figure 4c shows the plasma electron density distribution with the circular frustum substrate holder II. The high-density plasma region on the substrate holder extends to the left and right, changing the shape of the plasma sphere from circular to elliptical. This alteration may result in a more uniform deposition of polycrystalline diamond. However, it cannot be adjusted during the diamond growth process and requires further optimization. Figure 4d illustrates the plasma distribution with the adjustable cyclic-shaped substrate holder II. This holder retains the advantages shown in Figure 4c and exhibits a uniform and high-density area, facilitating the uniform deposition of polycrystalline diamond.

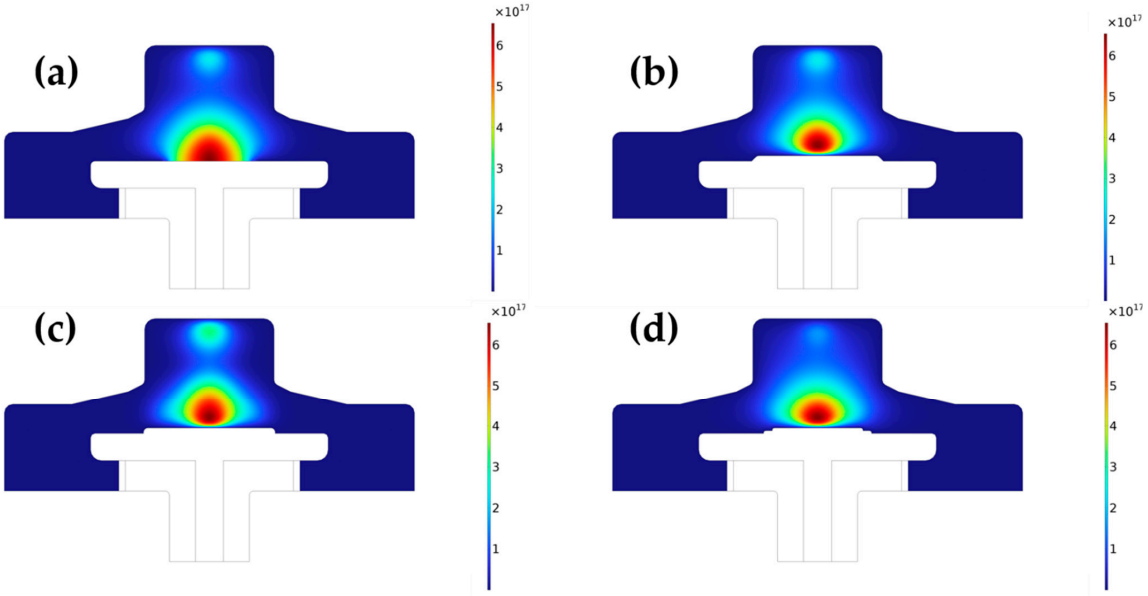

Figure 4. MPCVD equipment plasma electron density distribution map ($1/m^3$): (**a**) without substrate II, (**b**) trapezoidal, (**c**) circular frustum, and (**d**) adjustable cyclic shape.

3.3. Influence of the Substrate Holder on the Temperature of the Gas in the Cavity

Figure 5 shows the gas temperature distribution for different substrate holders. By comparing it with Figure 4, it is evident that gas temperature distribution correlates with plasma electron density distribution. As shown in Figure 5a, in the absence of substrate support II, a hat-shaped high-temperature zone will form in the plasma region. When the trapezoidal substrate holders are added, the high-temperature region becomes more dispersed, as seen in Figure 5b. In Figure 5c, the high-temperature region is slightly lower and spreads more towards the edges of the substrate holder. Figure 5d shows the broadest high-temperature region, indicating that the substrate holder design can maximize the area exposed to high temperatures, thereby improving the uniformity of diamond film deposition.

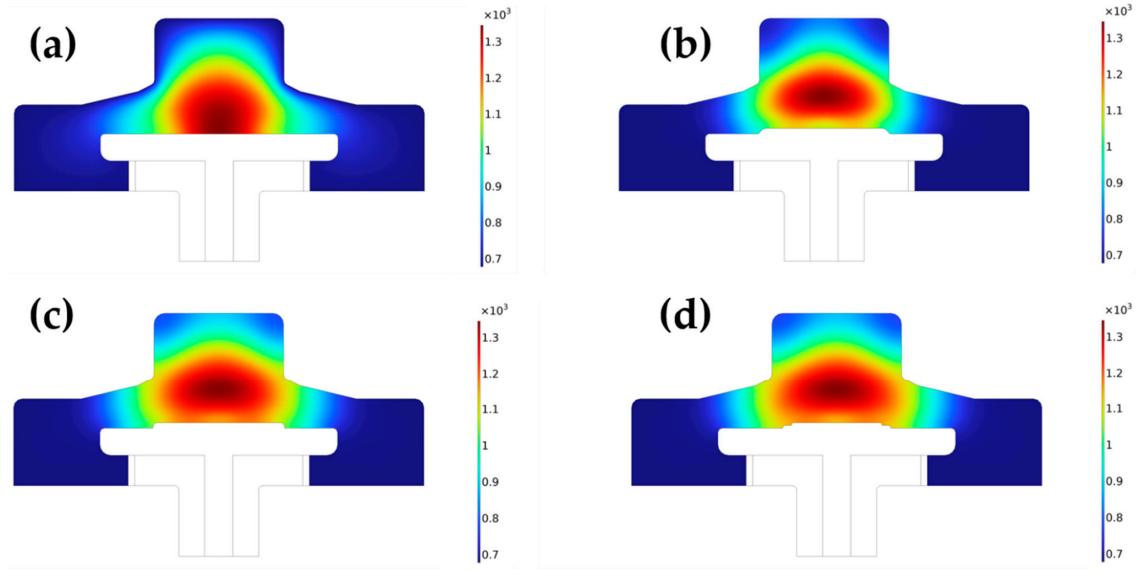

Figure 5. Temperature (K) distribution of plasma gas in MPCVD equipment: (**a**) without substrate II, (**b**) trapezoidal, (**c**) circular frustum, and (**d**) adjustable cyclic shape.

Figure 6 illustrates the number density distribution of H species along the central axis of the chamber under three different substrate holder configurations. The x-axis represents the height from the substrate surface. The figure reveals that the trend of the distribution curve varies with different substrate holders. Without a substrate holder, the number density generally increases with height. When a trapezoidal substrate holder is used, the H species number density is higher near the substrate surface and gradually decreases with increasing distance. In contrast, with the adjustable cyclic-shaped substrate holder, a uniform distribution of H species is observed within 10 mm from the substrate surface, and the overall trend shows a gradual decrease beyond this point. This uniform distribution supports the reliability of the proposed substrate holder design for producing high-quality diamond films.

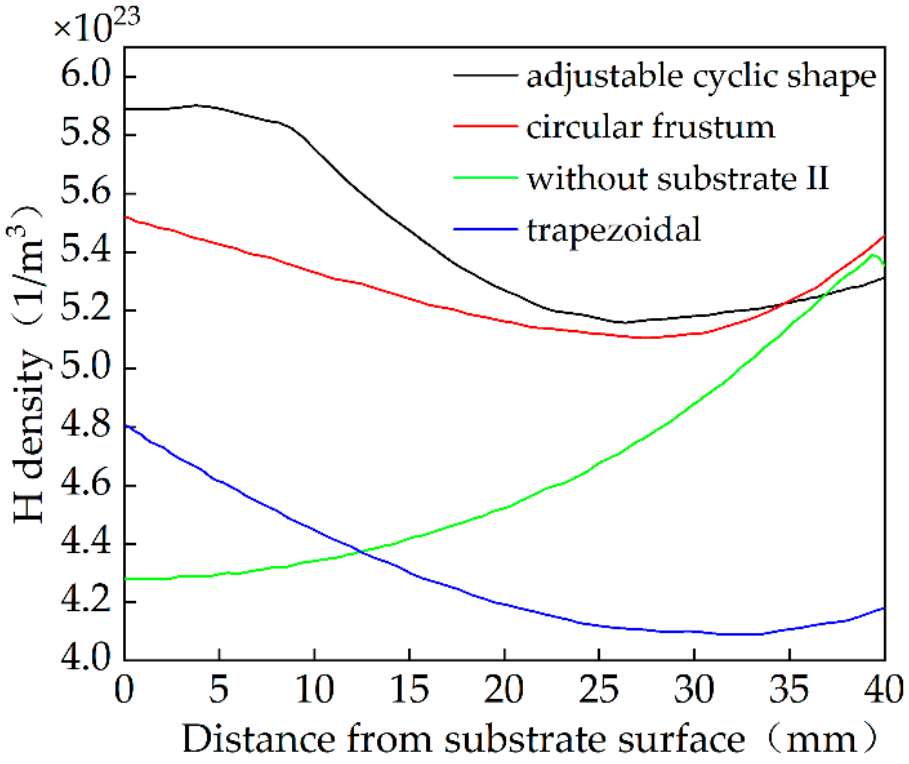

Figure 6. The number density distribution curve of substance H along the axis direction of the cavity.

3.4. Experimental Verification of Simulation Results

The actual MPCVD growth process is complex and requires experimental verification for an accurate simulation. Based on the simulation results, we manufactured three types of substrate holder II and placed them in a cavity for experimental testing. As shown in Figure 7, the actual plasmonic spheres generated using different substrate holders exhibited varying coverage and shapes. Figure 7a illustrates the trapezoidal substrate holder, in which the plasmonic sphere appears as a slightly curved elliptical shape with incomplete coverage. It is mainly concentrated in the center of the cavity with weak edges. Figure 7b shows the circular frustum substrate holder, where the plasma shape becomes more uniform, covering almost the entire top and bottom, and the brightness is more consistent. Figure 7c shows the adjustable cyclic shape, where the plasma appears flat and completely covers the substrate holder. These observations indicate that different substrate holders affect the plasma distribution and shape. Thus, optimization of the substrate holders can achieve improved plasma distribution and deposition effects. Additionally, it can be seen that the experimental plasma distribution results are largely consistent with the simulations.

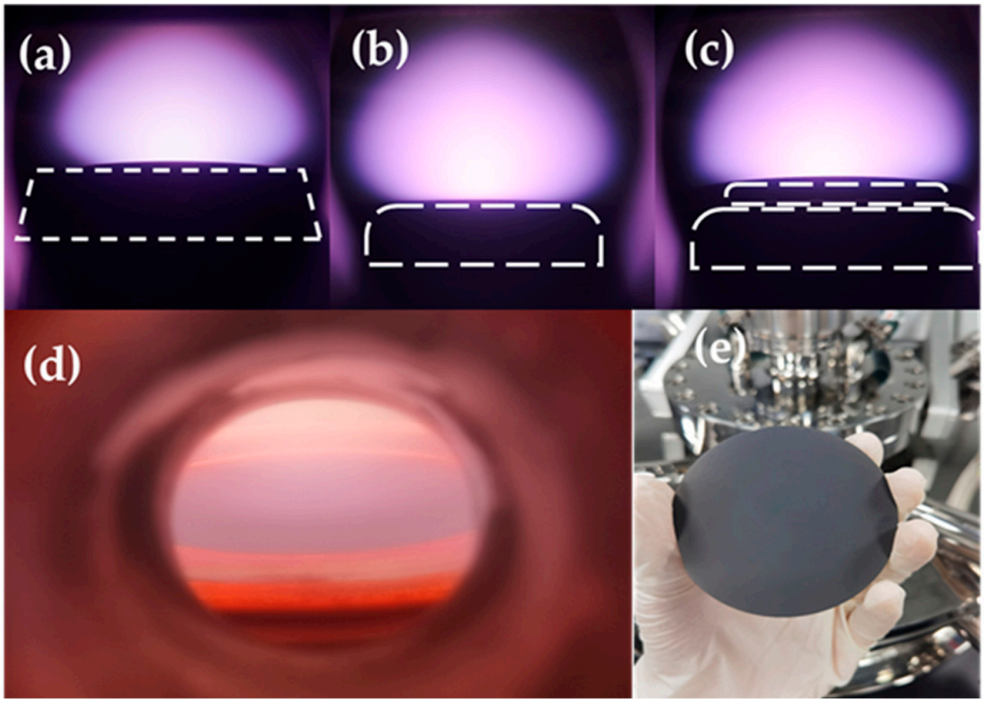

Figure 7. Plasma distribution diagram of the MPCVD device in a hydrogen atmosphere experiment: (**a**) trapezoidal, (**b**) circular frost, and (**c**) adjustable cyclic shape. (**d**) An actual image of polycrystalline diamond growth under an adjustable cyclic-shaped substrate holder. (**e**) Three inches of high-quality polycrystalline diamond growth under an adjustable cyclic-shaped substrate holder.

To verify the influence of the substrate holders, we used three types to analyze polycrystalline diamond films grown under identical parameters for four hours. The growth process using an adjustable cyclic substrate holder is illustrated in Figure 7d. The substrate holder turned bright red with plasma heating. Figure 7e shows the polycrystalline diamond thin film deposited in an adjustable cyclic-shaped substrate holder, which appears uniformly black. For comparison, we examined polycrystalline diamond films prepared using two other methods. Figure 8 shows the SEM images of these films. Figure 8a shows the results obtained using the trapezoidal substrate holder. The surface is not fully covered with polycrystalline diamond, displaying a graphite phase and 10-μm-sized polygonal diamond particles. Figure 8b shows complete coverage with a relatively small amount of graphite phase and a consistent structure within the region. Figure 8c shows that nearly full coverage of the surface was achieved. The polycrystalline diamond particles exhibited a uniform quadrilateral morphology with a lower growth rate than that shown in Figure 8b. This finding is consistent with those of other studies, suggesting that an excessively fast growth rate can reduce quality. The particle size distribution histograms indicate that the average particle sizes for the trapezoidal substrate holder, circular frustum, and adjustable cyclic shape are 4.24 μm, 4.49 μm, and 4.33 μm, respectively. The circular frustum exhibits the fastest growth rate and largest average size, while the adjustable cyclic shape results in the most uniform particle size distribution, leading to the highest-quality diamond growth. Consequently, we chose to deposit high-quality polycrystalline diamond films using the adjustable cyclic-shaped substrate holder [35].

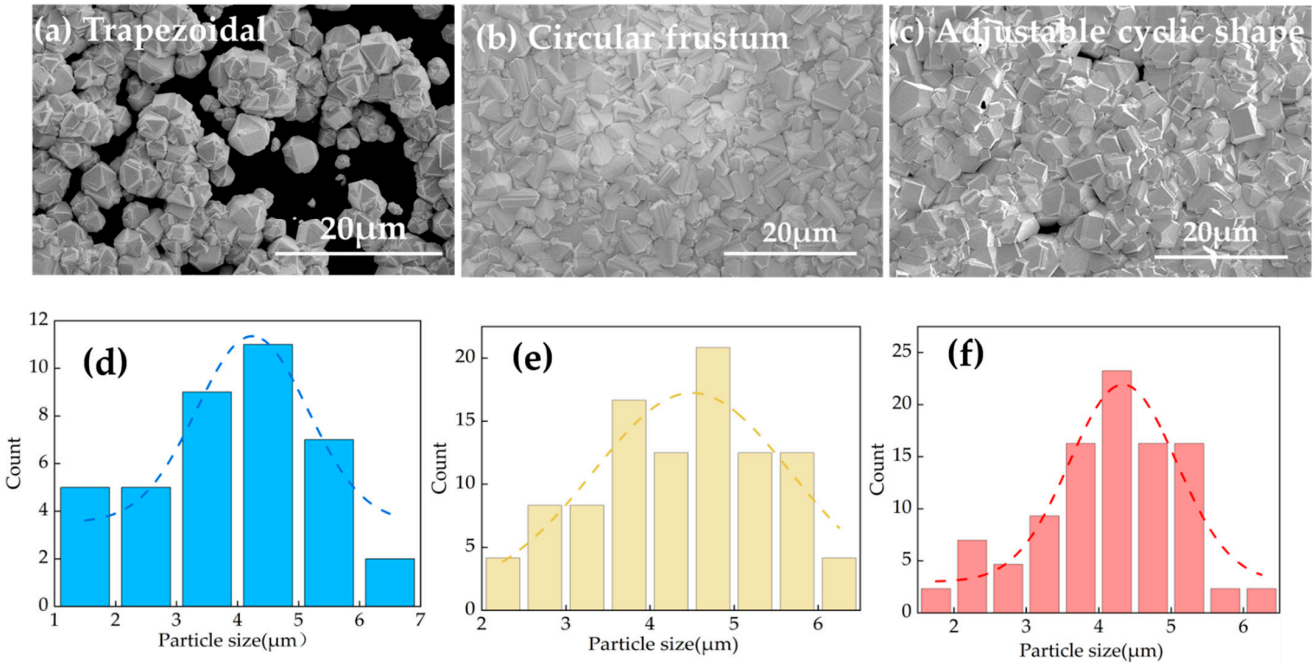

Figure 8. (**a**–**c**) The surface morphologies of polycrystalline diamond prepared on three different substrate supports and (**d**–**f**) the corresponding particle size distribution maps (The dashed line represents the Gaussian function fitted to obtain the normal distribution curve).

Temperature is also critical for polycrystalline diamond growth. We used infrared temperature measurements to monitor substrate growth through a viewing window at the top of the chamber. As shown in Figure 9, the center of the trapezoidal substrate holder has the highest temperature of 1136 K, while the lowest temperature at the edges is 935 K. This significant temperature difference leads to different diamond growth rates. Rapid changes in pressure and power can lead to silicon rupture. These results are consistent with the simulation results shown in Figure 5b, indicating that an inhomogeneous temperature field distribution is detrimental to the growth of polycrystalline diamond. In contrast, the temperature difference of the adjustable ring substrate holder is very small, which is consistent with the results in Figure 5d. Therefore, this study demonstrates the feasibility of the adjustable cyclic substrate holder and suggests a feasible route for growing large-scale high-quality polycrystalline diamond films.

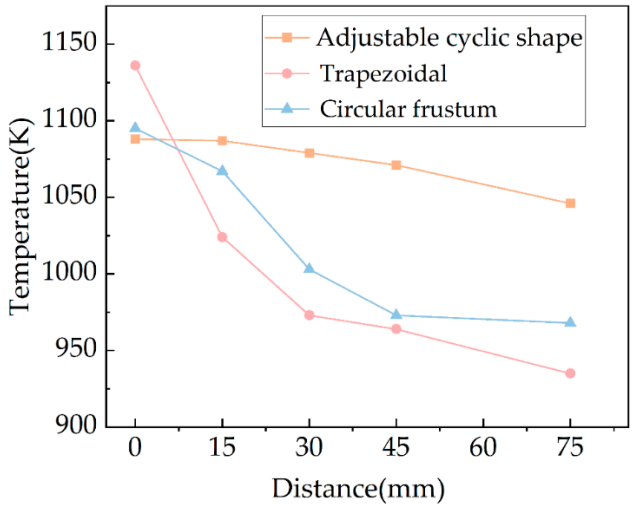

Figure 9. Temperature from the center of the substrate silicon wafer to the outside during growth of different substrate holders.

Additionally, to evaluate the quality of polycrystalline diamond produced by the three different substrate holders, Raman spectroscopy was conducted, as shown in Figure 10. The residual stress in the diamond films can be calculated based on the shift in the Raman peak using the following equation:

$$\sigma = m(\nu - \nu_0) \tag{11}$$

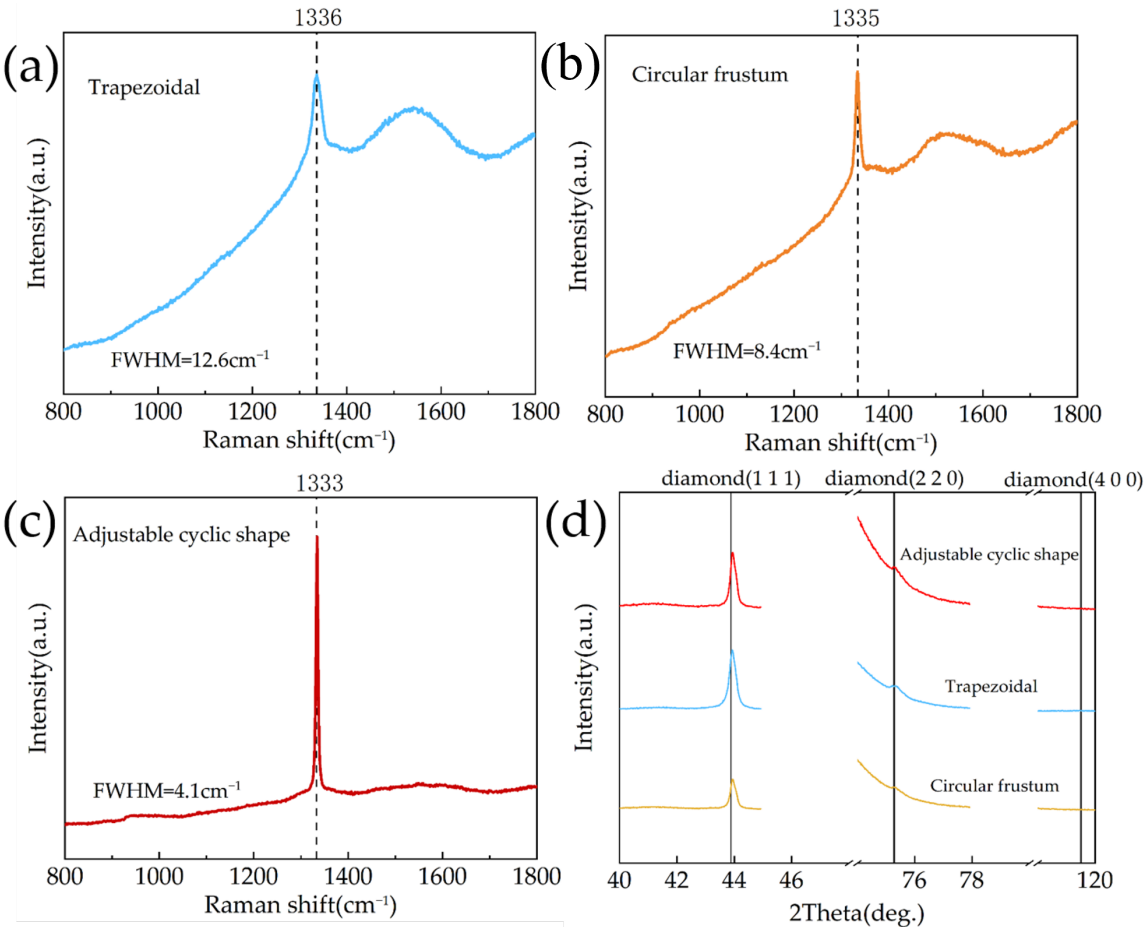

Figure 10. Raman spectra (**a**–**c**) and XRD diffraction patterns (**d**) of polycrystalline diamond prepared on different substrate supports.

In this equation, m is $-0.567\,\mathrm{GPa/cm^{-1}}$, ν_0 is the wavenumber of natural, stress-free diamond (1332 $\mathrm{cm^{-1}}$), and ν is the measured wavenumber of the diamond. Therefore, the residual stress in all samples predominantly manifests as compressive stress. Specifically, the trapezoidal sample exhibits a residual stress of 2.268 GPa, the circular frustum sample shows a stress of 1.701 GPa, and the adjustable cyclic-shaped sample presents a stress of 0.567 GPa. Additionally, the FWHM of the characteristic Raman peak, which is a critical parameter for assessing diamond quality, is 12.6 $\mathrm{cm^{-1}}$, 8.4 $\mathrm{cm^{-1}}$, and 4.1 $\mathrm{cm^{-1}}$, respectively, for these samples. In the XRD patterns, only the (111) and (220) diffraction peaks are observed, with the (400) peak displaying the highest intensity, as shown in Figure 10d. Notably, the adjustable cyclic-shaped substrate holder exhibits the lowest FWHM at 0.27°, indicating the highest crystal quality. This indicates that the shape of the substrate holder significantly impacts the quality of the diamond. Among the tested designs, the diamond produced using the adjustable cyclic-shaped substrate holder exhibited the highest quality.

Owing to the etching effect of hydrogen plasma on the graphite sp^2 phase, polycrystalline diamond can undergo high-quality growth [21]. In comparison, the trapezoidal substrate holder resulted in a larger graphite phase. The conical substrate holder also

contained some graphite phase. This is due to the rapid growth of diamond, which leads to the deposition of graphite that is not completely etched away. Overall, using an adjustable circular substrate holder ensures a uniform distribution of the electric field, plasma electron density, and temperature, making it feasible to grow high-quality three-inch polycrystalline diamond. The experimental results are consistent with the simulation results, validating the reliability of the simulation method used in this study.

4. Conclusions

This study investigates the impact of three distinct substrate holder shapes—trapezoidal, circular frustum, and adjustable cyclic—on the quality of polycrystalline diamond films. Using a frequency-domain transient solver, simulations were conducted to model the electric field and plasma distribution for each holder shape. Changes in the holder shape resulted in corresponding variations in the electric field and plasma distribution within the chamber. The trapezoidal shape enhanced secondary plasma formation, but the plasma ball did not fully cover the surface. The circular frustum shape reduced secondary plasma, minimizing energy loss and achieving the highest growth rate. However, it also introduced a graphite phase, which diminished the quality of the polycrystalline diamond films. To overcome these challenges, an adjustable cyclic substrate holder was proposed. This design suppressed secondary plasma, and the gas temperature distribution above the substrate evolved from a sombrero shape to a more uniform profile, improving the uniformity of temperature and hydrogen species density. Infrared temperature measurements showed that the trapezoidal holder exhibited a significant temperature gradient from the center to the edge, which hindered uniform growth. In contrast, the adjustable cyclic shape demonstrated the smallest temperature variation across the substrate surface, leading to more uniform growth. The polycrystalline diamond films deposited using the adjustable cyclic holder exhibited the lowest residual stress (0.567 GPa) and the narrowest FWHM of 4.1 cm^{-1}, predominantly oriented along the (111) crystal plane. The experimental results validated the simulation findings and confirmed the effectiveness of the adjustable cyclic substrate holder. This design offers a viable approach to enhancing the performance of existing MPCVD systems, facilitating the production of high-quality, large-area polycrystalline diamond films.

Author Contributions: Conceptualization, S.W.; methodology, S.W., J.L. and K.G.; software, S.W., J.Z. and K.G.; formal analysis, S.W.; investigation, K.G.; data curation, L.L. and L.H.; writing—original draft, S.W. and K.G.; writing—review and editing, J.B., K.G., C.Z. and Q.W.; project administration, K.G., Q.W. and J.B.; funding acquisition, K.G. and Q.W. All authors have read and agreed to the published version of the manuscript.

Funding: This research was funded by the Guangdong Basic and Applied Basic Research Foundation, China (Grant No. 2023B1515120033), the National Natural Science Foundation of China (Grant Nos. 52102037, 52302037), the General Program of the Chongqing Municipal Science and Technology Commission (Grant No. CSTB2022NSCQ-MSX0495), the Chongqing Municipal Education Commission Science and Technology Research Project (Grant Nos. KJQN202000742, KJQN202100733), and the Research and Innovation Program for Graduate Students in Chongqing (Grant No. CYS240525).

Informed Consent Statement: Not applicable.

Data Availability Statement: The original contributions presented in this study are included in the article; further inquiries can be directed to the corresponding authors.

Acknowledgments: Grateful acknowledgment is extended to the Jihua Laboratory Testing Center for their assistance with the SEM images and Raman spectroscopy. Appreciation is also given to Jingming Zhu and Jiafeng Li for their valuable help in conducting numerical simulations and experiments.

Conflicts of Interest: The authors declare no conflicts of interest.

References

1. Sun, D.-R.; Wang, G.; Li, Y.; Yu, Y.; Shen, C.; Wang, Y.; Lu, Z. Laser drilling in silicon carbide and silicon carbide matrix composites. *Opt. Laser Technol.* **2024**, *170*, 110166. [CrossRef]
2. Castelletto, S.; Boretti, A. Gallium Nitride Nanomaterials and Color Centers for Quantum Technologies. *ACS Appl. Nano Mater.* **2024**, *7*, 5862–5877. [CrossRef]
3. Yang, H.; Sun, J.; Wang, H.; Li, H.; Yang, B. A review of oriented wurtzite-structure aluminum nitride films. *J. Alloys Compd.* **2024**, *989*, 174330. [CrossRef]
4. Chen, J.; Du, X.; Luo, Q.; Zhang, X.; Sun, P.; Zhou, L. A Review of Switching Oscillations of Wide Bandgap Semiconductor Devices. *IEEE Trans. Power Electron.* **2020**, *35*, 13182–13199. [CrossRef]
5. Mazumder, S.K.; Voss, L.F.; Dowling, K.M.; Conway, A.; Hall, D.; Kaplar, R.J.; Pickrell, G.W.; Flicker, J.; Binder, A.T.; Chowdhury, S.; et al. Overview of Wide/Ultrawide Bandgap Power Semiconductor Devices for Distributed Energy Resources. *IEEE J. Emerg. Sel. Top. Power Electron.* **2023**, *11*, 3957–3982. [CrossRef]
6. Zhang, C.; Vispute, R.D.; Fu, K.; Ni, C. A review of thermal properties of CVD diamond films. *J. Mater. Sci.* **2023**, *58*, 3485–3507. [CrossRef]
7. Jia, X.; Wei, J.; Huang, Y.; Shao, S.; An, K.; Kong, Y.; Liu, J.; Chen, L.; Li, C. Fabrication of low stress GaN-on-diamond structure via dual-sided diamond film deposition. *J. Mater. Sci.* **2021**, *56*, 6903–6911. [CrossRef]
8. Jaeger, W. CVD Diamond Films—Synthesis, Microstructure, Applications. *Microsc. Microanal.* **2017**, *23* (Suppl. S1), 2260–2261. [CrossRef]
9. Siyi, C.; Juping, T.; Ke, H.; Siwu, S.; Zhiliang, Y.; Peng, L.; Jinlong, L.; Liangxian, C.; Junjun, W.; Kang, A.; et al. Uniform Growth of Two-inch MPCVD Optical Grade Diamond Film. *J. Inorg. Mater.* **2023**, *38*, 1413–1419.
10. Wang, Q.; Wu, G.; Liu, S.; Gan, Z.; Yang, B.; Pan, J. Simulation-Based Development of a New Cylindrical-Cavity Microwave-Plasma Reactor for Diamond-Film Synthesis. *Crystals* **2019**, *9*, 320. [CrossRef]
11. Yu, L.; Zhang, Y.Q.; Jin, X.R.; Lee, Y.P. Dual-band unidirectional reflectionless phenomenon based on high-order plasmon resonators in plasmonic waveguide system. *J. Nonlinear Opt. Phys. Mater.* **2022**, *31*, 2350002. [CrossRef]
12. Hong, S.P.; Lee, K.-i.; You, H.J.; Jang, S.O.; Choi, Y.S. Scanning Deposition Method for Large-Area Diamond Film Synthesis Using Multiple Microwave Plasma Sources. *Nanomaterials* **2022**, *12*, 1959. [CrossRef] [PubMed]
13. Mukherjee, D.; Oliveira, F.; Trippe, S.C.; Rotter, S.; Neto, M.; Silva, R.; Mallik, A.K.; Haenen, K.; Zetterling, C.-M.; Mendes, J.C. Deposition of diamond films on single crystalline silicon carbide substrates. *Diam. Relat. Mater.* **2020**, *101*, 107625. [CrossRef]
14. Bolshakov, A.P.; Ralchenko, V.G.; Yurov, V.Y.; Shu, G.; Bushuev, E.V.; Khomich, A.A.; Ashkinazi, E.E.; Sovyk, D.N.; Antonova, I.A.; Savin, S.S.; et al. Enhanced deposition rate of polycrystalline CVD diamond at high microwave power densities. *Diam. Relat. Mater.* **2019**, *97*, 107466. [CrossRef]
15. Wang, H.; Wang, C.; Wang, X.; Sun, F. Effects of carbon concentration and gas pressure with hydrogen-rich gas chemistry on synthesis and characterizations of HFCVD diamond films on WC-Co substrates. *Surf. Coat. Technol.* **2021**, *409*, 126839. [CrossRef]
16. Yudin, I.B.; Emelyanov, A.A.; Plotnikov, M.Y.; Rebrov, A.K.; Timoshenko, N.I. Influence of nitrogen on the synthesis of diamonds during gas-jet HWCVD deposition. *Fuller. Nanotub. Carbon Nanostructures* **2022**, *30*, 126–132. [CrossRef]
17. Wang, H.; Shen, X.; Wang, X.; Sun, F. Simulation and experimental researches on the substrate temperature distribution of the large-capacity HFCVD setup for mass-production of diamond coated milling tools. *Diam. Relat. Mater.* **2020**, *101*, 107610. [CrossRef]
18. Yang, Z.; Liu, Y.; Guo, Z.; Wei, J.; Liu, J.; Chen, L.; Li, C. Deposition of uniform diamond films on three dimensional Si spheres by using faraday cage in MPCVD reactor. *Diam. Relat. Mater.* **2024**, *142*, 110767. [CrossRef]
19. Sedov, V.; Martyanov, A.; Altakhov, A.; Popovich, A.; Shevchenko, M.; Savin, S.; Zavedeev, E.; Zanaveskin, M.; Sinogeykin, A.; Ralchenko, V.; et al. Effect of Substrate Holder Design on Stress and Uniformity of Large-Area Polycrystalline Diamond Films Grown by Microwave Plasma-Assisted CVD. *Coatings* **2020**, *10*, 939. [CrossRef]
20. Curto, S.; Taj-Eldin, M.; Fairchild, D.; Prakash, P. Microwave ablation at 915 MHz vs 2.45 GHz: A theoretical and experimental investigation. *Med. Phys.* **2015**, *42*, 6152–6161. [CrossRef]
21. Yang, D.; Guo, L.; Wang, B.; Jin, S.; Zhu, J.; Zhai, M. Hydrogen plasma characteristics in a microwave chemical vapor deposition chamber. *Mater. Sci. Eng. B* **2023**, *292*, 116422. [CrossRef]
22. Liu, S.; Jiang, L.; Li, H.; Zhao, J.; Wang, K.; Wang, H.; Li, T.; Zhou, Y.; Ghannouchi, F.M.; Hu, B. Design of a coaxial and compact TM01–TE01 mode converter based on helical corrugated waveguide for high-power microwave system. *AIP Adv.* **2022**, *12*, 115120. [CrossRef]
23. Xiao, R.; Chen, K.; Wang, H.; Wang, D.; Shi, Y.; Gao, L. Theoretical calculation and particle-in-cell simulation of a multi-mode relativistic backward wave oscillator operating at low magnetic field. *Phys. Plasmas* **2022**, *29*, 043103. [CrossRef]
24. Weng, J.; Xiong, L.W.; Wang, J.H.; Dai, S.Y.; Man, W.D.; Liu, F. Investigation of depositing large area uniform diamond films in multi-mode MPCVD chamber. *Diam. Relat. Mater.* **2012**, *30*, 15–19. [CrossRef]
25. An, K.; Chen, L.; Liu, J.; Zhao, Y.; Yan, X.; Hua, C.; Guo, J.; Wei, J.; Hei, L.; Li, C.; et al. The effect of substrate holder size on the electric field and discharge plasma on diamond-film formation at high deposition rates during MPCVD. *Plasma Sci. Technol.* **2017**, *19*, 095505. [CrossRef]

26. Zhao, W.; Teng, Y.; Tang, K.; Zhu, S.; Yang, K.; Duan, J.; Huang, Y.; Chen, Z.; Ye, J.; Gu, S. Significant suppression of residual nitrogen incorporation in diamond film with a novel susceptor geometry employed in MPCVD. *Chin. Phys. B* **2022**, *31*, 118102. [CrossRef]
27. Hassouni, K.; Grotjohn, T.A.; Gicquel, A. Self-consistent microwave field and plasma discharge simulations for a moderate pressure hydrogen discharge reactor. *J. Appl. Phys.* **1999**, *86*, 134–151. [CrossRef]
28. Li, X.-J.; Zhou, S.; Chen, G.; Wang, D.-S.; Pei, N.; Guo, H.-L.; Nie, F.-M.; Zhang, X.; Feng, S. Systematic research on the performance of self-designed microwave plasma reactor for CVD high quality diamond. *Def. Technol.* **2018**, *14*, 373–379. [CrossRef]
29. Zhang, Y.; Yu, S.; Gao, J.; Ma, Y.; He, Z.; Hei, H.; Zheng, K. Design and simulation of a novel MPCVD reactor with three-cylinder cavity. *Vacuum* **2022**, *200*, 111055. [CrossRef]
30. Weng, J.; Liu, F.; Wang, Z.T.; Guo, N.F.; Fan, F.Y.; Yang, Z.; Wang, J.B.; Wang, H.; Xiong, L.W.; Zhao, H.Y.; et al. Investigation on the preparation of large area diamond films with 150–200 mm in diameter using 915 MHz MPCVD system. *Vacuum* **2023**, *217*, 112543. [CrossRef]
31. Harris, S.J.; Goodwin, D.G. Growth on the reconstructed diamond (100) surface. *J. Phys. Chem.* **1993**, *97*, 23–28. [CrossRef]
32. Silva, F.; Hassouni, K.; Bonnin, X.; Gicquel, A. Microwave engineering of plasma-assisted CVD reactors for diamond deposition. *J. Phys. Condens. Matter* **2009**, *21*, 364202. [CrossRef] [PubMed]
33. Hassouni, K.; Silva, F.; Gicquel, A. Modelling of diamond deposition microwave cavity generated plasmas. *J. Phys. D Appl. Phys.* **2010**, *43*, 153001. [CrossRef]
34. Yang, B.; Shen, S.; Zhang, L.; Shen, Q.; Zhang, R.; Zhang, Y.; Gan, Z.; Liu, S. Study on diamond temperature stability during long-duration growth via MPCVD under the influence of thermal contact resistance. *J. Appl. Crystallogr.* **2022**, *55*, 240–246. [CrossRef]
35. Chen, K.; Tao, T.; Hu, W.; Ye, Y.; Zheng, K.; Ye, J.; Zhi, T.; Wang, X.; Liu, B.; Zhang, R. High-speed growth of high-quality polycrystalline diamond films by MPCVD. *Carbon Lett.* **2023**, *33*, 2003–2010. [CrossRef]